Electronic Supplementary Material (ESI) for Nanoscale.
This journal is © The Royal Society of Chemistry 2014

High-yield fabrication of nm-size gaps in monolayer CVD graphene†

Cornelia Nef,[*a] László Pósa,[b] Péter Makk,[a,b] Wangyang Fu,[a] András Halbritter,[b] Christian Schönenberger,[a] and Michel Calame[*a]

Received Xth XXXXXXXXXX 20XX, Accepted Xth XXXXXXXXX 20XX
First published on the web Xth XXXXXXXXXX 200X
DOI: 10.1039/b000000x

Supporting information

Temperature dependence of the Si Raman peak position

The shift of the Si peak at ≈ 520 1/cm was fitted with a model for inelastic scattering based on three phonon processes Cowley (1965); Balkanski *et al.* (1983).

$$Pos(Si) = \omega_0 + C\left(1 + \frac{2}{e^x - 1}\right), \tag{1}$$

with $x = \hbar\omega_0/k_B T$, where ω_0 is the Raman frequency shift at 0 K, C is a constant, $\hbar$ is the reduced Planck constant, k_B is the Boltzmann constant and T is the temperature. We found values of $\omega_0 = 536.7$ 1/cm and $C = -5.07$ 1/cm. The data and the fit are shown in figure 2a), low left inset in the main article.

0.1 Correction of the focus drift

As control measurements showed a shift of the peak positions with defocusing (figure 1 blue solid squares), we had to correct for this effect to be able to deduce the temperature of the graphene. This shift follows a Lorentzian, which is shown in figure 1 (black dashed line). As we did not observe a change of the area of the 2D peak with temperature this was used to calculate the actual focus position. The dependence of the peak area on the focus can be derived from the intensity of a

0 † Electronic Supplementary Information (ESI) available: Further information is provided regarding the temperature dependence of the Si Raman peak at ≈ 520 1/cm, a description of the procedure to correct for the focus drift and details of the Simmons fitting procedure. See DOI: 10.1039/b000000x/

0 [a] *Department of Physics, University of Basel, Klingelbergstrasse 82, CH-4056 Basel, Switzerland. Fax: +41 61 267 37 84; Tel: +41 61 267 37 80; E-mail: c.nef@unibas.ch; michel.calame@unibas.ch*
0 [b] *Department of Physics, Budapest University of Technology and Economics and MTA-BME Condensed Matter Research Group, Budafoki ut 8, 1111 Budapest, Hungary.*

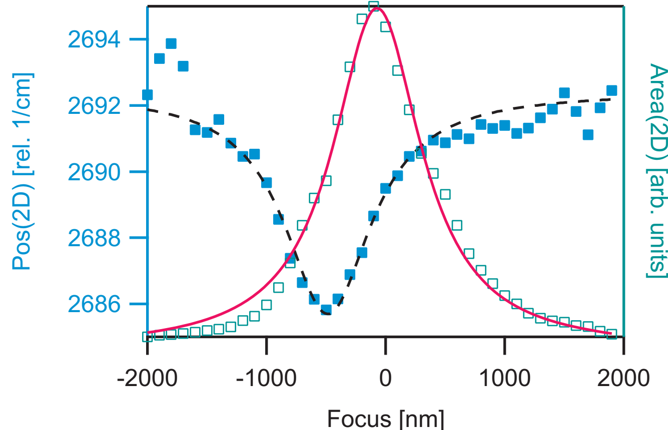

Fig. 1: Dependence of the graphene 2D peak position (blue solid squares) and area (turquoise open squares) on the focus position. A Lorentzian fit to the peak position and a fit of equation 2 (black dashed line) are shown as well.

Gaussian beam

$$I(x) = \frac{I_0}{1 + \left(\frac{x - x_0}{z_R}\right)^2}, \tag{2}$$

where I_0 is the intensity at optimal focus, x_0 is the position of the optimal focus, x is the actual focus position and z_R is the distance from the optimal focus where only the half intensity of the beam is left. The area of the 2D peak with changing focus and a fit to equation 2 are shown in figure 1 (turquoise open squares, pink solid line). Note that the ideal focus point (area is maximal) does not correspond to the point of lowest 2D phonon energy.

AFM imaging of the gaps

We performed a topological analysis of the freshly burned gaps using AFM. For this we used a Dimension 3100 (Veeco, USA) in combination with PPP-NCHR cantilevers (Nanosensors, Switzerland). The measurements were performed in ambient conditions, where atomic resolution imaging is not possible. This analysis provides an upper limit for the gap size. An image of a typical device is shown in figure 2 left panel. A cross section through the graphene channel (middle panel, turquoise line) gives an apparent graphene thickness of 0.7 nm, in agreement with the thickness for monolayer graphene reported in the literature Novoselov *et al.* (2005); Ishigami *et al.* (2007). We measured cross sections along different positions on the gap (two examples shown in the right panel). The gap size is measured at the graphene height

(determined from the cross section over the graphene channel). The narrowest slit was found to be ≈ 4.5 nm wide. These measurements also show that the gap size is not homogeneous along the slit.

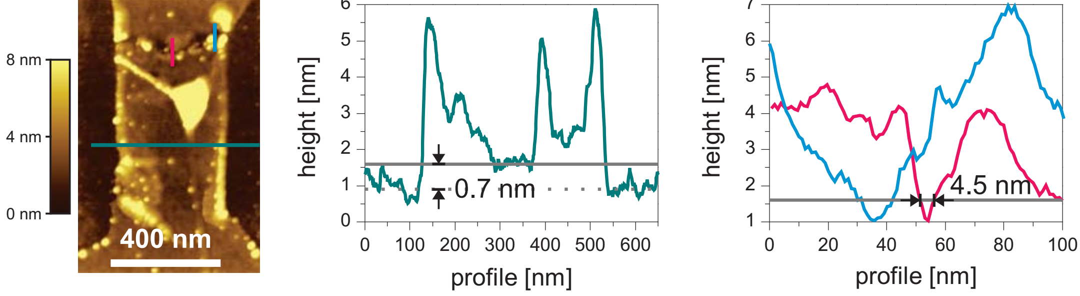

Fig. 2: AFM image and height profiles across the graphene channel and over the gap. The gap size is estimated to be 4.5 nm wide.

Details of the Simmons fitting procedure

The Simmons model describes tunneling through a potential barrier of arbitrary shape (see figure 3a) by the following equation Simmons (1963)

$$J = J_0 \Bigg\{ \underbrace{\overline{\Phi} \exp\left(\frac{-2d\beta}{\hbar} \sqrt{2m} \sqrt{\overline{\Phi}} \right)}_{J_L/J_0} - \underbrace{(\overline{\Phi} + eV) \exp\left(\frac{-2d\beta}{\hbar} \sqrt{2m} \sqrt{\overline{\Phi} + eV} \right)}_{J_R/J_0} \Bigg\} \qquad (3)$$

$$\text{with} \qquad J_0 = \frac{e}{4\pi^2 \hbar d^2 \beta^2},$$

where J is the current density, e is the elementary charge, $\hbar$ is the reduced Planck's constant, $\overline{\Phi}$ is the mean barrier height, m is the electron mass, V is the potential applied and β is a correction factor which is 1 to a good approximation and will be neglected from now on.

We assume a rectangular barrier with $V < \Phi_b/e$ (see figure 3c)), where Φ_b is the height of the rectangular barrier. In this case $\overline{\Phi} = \Phi_b - eV/2$ using 3 we can calculate

the current I as follows

$$I = \frac{Ae}{4\pi^2 \hbar d^2} \left\{ \left(\Phi_b - \frac{eV}{2} \right) \exp\left(\frac{-2d}{\hbar} \sqrt{2m} \sqrt{\Phi_b - \frac{eV}{2}} \right) - \left(\Phi_b + \frac{eV}{2} \right) \exp\left(\frac{-2d}{\hbar} \sqrt{2m} \sqrt{\Phi_b + \frac{eV}{2}} \right) \right\}, \quad (4)$$

where A is the area of the junction. For really small bias ($V \approx 0$, see figure 3b)) This reduces to

$$I \propto V \exp\left(\frac{-2d\sqrt{2m\Phi_b}}{\hbar} \right). \quad (5)$$

At high applied bias ($V > \Phi_b/e$) (see figure 3d)), the barrier shape changes from trapezoidal to triangular, what is also known as field emission or Fowler-Nordheim tunneling, and this formula is not valid anymore. Thus beforehand of the fitting we need to find the bias at which this transition takes place. One method to do this is transition voltage spectroscopy Beebe *et al.* (2006). The current flowing in figure 3d) can be described through

$$\ln\left(\frac{I}{V^2} \right) \propto -\frac{4d\sqrt{2m\Phi_b^3}}{3\hbar e} \left(\frac{1}{V} \right). \quad (6)$$

A plot of $\ln(I/V^2)$ versus $1/V$ will yield a linear decrease for this regime, but a logarithmic growth for the regime where $V \approx 0$. The transition between them corresponds to the voltage required to change the shape of the barrier from trapezoidal to

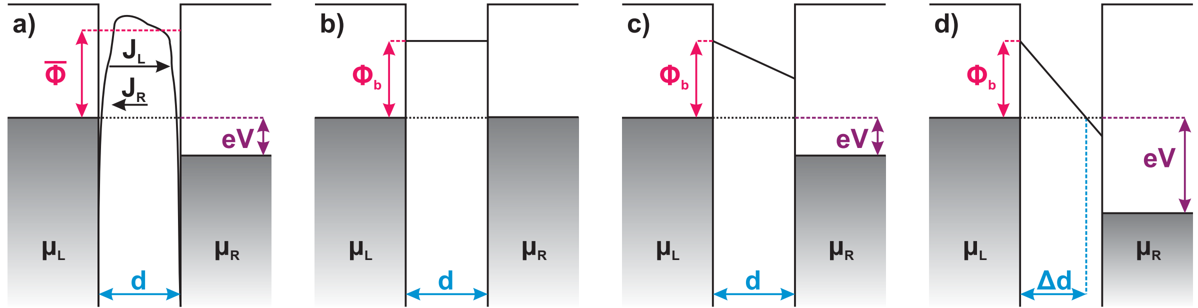

Fig. 3: Potential barrier with thickness d between to electrodes with the same work function, μ_L and μ_R are the chemical potentials. a) General barrier with the mean height $\overline{\Phi}$ and an applied potential of eV. The current density to the left J_L and to the right J_R are shown in equation 3. b) Rectangular barrier with height Φ_b and $V = 0$, c) $eV < \Phi_b$ and d) $eV > \Phi_b$, this leads to an effective barrier width Δd.

triangular. Thus plotting the $I-V$ curves in this way allows us to define a voltage regime, where a fit to equation 4 is appropriate. Figure 4a) shows this plot for the same tunneling curve as shown in figure 1d) in the main text. It shows a minimum at 2.5 V^{-1} leading to a transition voltage of 0.4 V. Figure 4b) shows the same tunneling curve (black) and a fit to equation 4 (pink). The values deduced from this fit are as follows: $A = 0.35$ nm^2, $d = 1.3$ nm and $\Phi_b = 0.26$ eV. The parameters A and Φ_b are quite sensitive to changes in the fitting range or the initial parameter set, but d is more robust.

We now also look at two additional devices showing different resistances than device 1. The resistance of the devices is determined from a linear fit to the low bias region (± 0.3 V). We obtain 19 GΩ and 100 GΩ for devices 2 and 3, respectively. The fitting region is again determined by V_T deduced from a Fowler-Nordheim plot. For the curves presented, we find $V_T = 0.6$ for device 2 and $V_T = 1.25$ V for device 3. The fits with free parameters and small initial $A_\square$ to the three curves are shown in figure 4. The corresponding fit parameters are given in table 1 for all three devices. For these fits, d is about the same for all devices. The difference in resistance R between the junctions is accounted for by changes in A. For all three devices, A is small

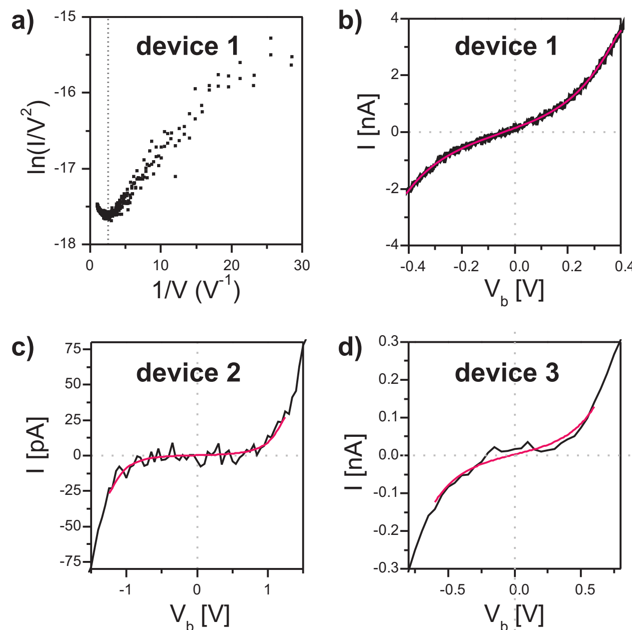

Fig. 4: a) I-V curve from figure 3d) of the main text plotted as $\ln(I/V^2)$ versus $1/V$ to determine the transition voltage and b) same I-V curve (black) with fit to equation 4 (pink) for ± 0.4 V. c) and d) show I-V curves for two different devices.

as compared to the maximum possible area of $\approx 100\,\mathrm{nm}^2$ in our case (constriction width times atom diameter). This could indicate that the gap is not homogeneous in width over the gap length, which is in agreement with the analysis of the gaps by AFM. However, the area A derived for device 3 is less than $1\,\text{Å}^2$ which is not realistic. One would expect Φ_b to maximally be the work function of graphite, which is 5 eV. We however obtain much lower values for Φ_b. This has been observed as well for multilayer graphene tunnel junctions Prins *et al.* (2011) and electromigrated gold junctions Mangin *et al.* (2009) and has been attributed to the presence of adsorbates or defects.

To demonstrate the robustness of d, we fit the curves to the Simmons model for a fixed area. For this we choose either $A = 100\,\mathrm{nm}^2$, which is approximately the maximum possible area for our devices or $A = 0.01\,\mathrm{nm}^2$, which would be comparable to the size of a single atom. Even with these extreme assumptions for A and letting d and Φ_b free, d remains between 0.4 nm and 1.9 nm for all three devices. To test the robustness of d further, we additionally fix Φ_b at either 5 eV (approximately the work function of graphite) or at eV_T. For an energy barrier smaller than eV_T, the Simmons model would not be appropriate anymore. For these fits we get values for d between 0.3 nm and 2.2 nm. Overall, although this procedure can not provide a true physical value, it allows to determine a limit for the gap size, being between 0.3 nm and 2.2 nm. A narrow distribution of the gap size is expected as the current depends exponentially on the distance between the electrodes. A change in the gap size would lead to a much larger change in the tunnel current and it would not be measurable anymore for large d.

Table 1: Fit parameters for the devices shown in figure 4. The resistance obtained from a linear fit (±0.3 V) and the threshold voltage (V_T) as derived from transition voltage spectroscopy are given in the top line. The V_T was used as the respective limit for the Simmons fits.

device 1: $R = 220$ MΩ, $V_T = 0.40$ V			
fixed parameters:	A	Φ_b	d
none	0.35 nm^2	0.26 eV	1.3 nm
A	100 nm^2	0.58 eV	1.6 nm
A	0.01 nm^2	1.05 eV	0.4 nm
A, Φ_b	100 nm^2	5 eV	0.6 nm
A, Φ_b	0.01 nm^2	5 eV	0.3 nm
A, Φ_b	100 nm^2	0.4 eV	2.1 nm
A, Φ_b	0.01 nm^2	0.4 eV	0.5 nm
device 2: $R = 19$ GΩ, $V_T = 0.60$ V			
fixed parameters:	A	Φ_b	d
none	0.02 nm^2	0.35 eV	1.3 nm
A	100 nm^2	0.78 eV	1.9 nm
A	0.01 nm^2	0.34 eV	1.2 nm
A, Φ_b	100 nm^2	5 eV	0.8 nm
A, Φ_b	0.01 nm^2	5 eV	0.4 nm
A, Φ_b	100 nm^2	0.6 eV	2.2 nm
A, Φ_b	0.01 nm^2	0.6 eV	0.9 nm
device 3: $R = 100$ GΩ, $V_T = 1.25$ V			
fixed parameters:	A	Φ_b	d
none	0.002 nm^2	0.65 eV	1.2 nm
A	100 nm^2	1.35 eV	1.8 nm
A	0.01 nm^2	0.81 eV	1.3 nm
A, Φ_b	100 nm^2	5 eV	0.9 nm
A, Φ_b	0.01 nm^2	5 eV	0.5 nm
A, Φ_b	100 nm^2	1.25 eV	1.9 nm
A, Φ_b	0.01 nm^2	1.25 eV	1.0 nm

References

1 R. A. Cowley, *J. Phys. (Paris)*, 1965, **26**, 659–667.

2 M. Balkanski, R. F. Wallis and E. Haro, *Phys. Rev. B*, 1983, **28**, 1928–1934.

3 K. S. Novoselov, D. Jiang, F. Schedin, T. J. Booth, V. V. Khotkevich, S. V. Morozov and a. K. Geim, *PNAS*, 2005, **102**, 10451–3.

4 M. Ishigami, J. H. Chen, W. G. Cullen, M. S. Fuhrer and E. D. Williams, *Nano Lett.*, 2007, **7**, 1643–8.

5 J. G. Simmons, *J. Appl. Phys.*, 1963, **34**, 1793.

6 J. Beebe, B. Kim, J. Gadzuk, C. Daniel Frisbie and J. Kushmerick, *Phys. Rev. Lett.*, 2006, **97**, 026801.

7 F. Prins, A. Barreiro, J. W. Ruitenberg, J. S. Seldenthuis, N. Aliaga-Alcalde, L. M. K. Vandersypen and H. S. J. van der Zant, *Nano Lett.*, 2011, **11**, 4607–11.

8 A. Mangin, A. Anthore, M. L. Della Rocca, E. Boulat and P. Lafarge, *Phys. Rev. B*, 2009, **80**, 235432.